

B15



C.E. SACLAY
DSM

DAPNIA-SPhN 94-25

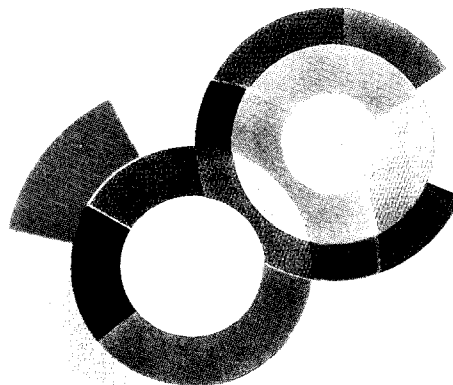
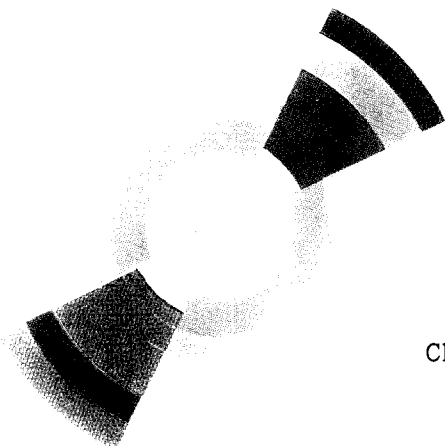
no 8429



CERN LIBRARIES, GENEVA



P00024355



CEA/DAPNIA/SPhN 94 25

05/1994

A NEW ISOMERIC STATE IN ^{65}Ni

J. Blons, D. Goutte, A. Leprêtre,
R. Létourneau, R. Lucas, V. Méot, D. Paya,
X.H. Phan, J. Girard, G. Barreau,
T.P. Doan, G. Pedemay, Ph. Dessagne,
Ch. Miehé

DAPNIA

Le DAPNIA (Département d'Astrophysique, de physique des Particules, de physique Nucléaire et de l'Instrumentation Associée) regroupe les activités du Service d'Astrophysique (SAp), du Département de Physique des Particules Élémentaires (DPhPE) et du Département de Physique Nucléaire (DPhN).

Adresse : DAPNIA, Bâtiment 141
CEA Saclay
F - 91191 Gif-sur-Yvette Cedex

Soumis pour publication dans

Nuclear Physics A

A NEW ISOMERIC STATE IN ^{65}Ni .

J. BLONS, D. GOUTTE, A. LEPRETRE, R. LETOURNEAU,
R. LUCAS, V. MEOT, D. PAYA and X.H. PHAN

Commissariat à l'énergie atomique, DAPNIA / SPhN, CE Saclay, 91191 Gif sur Yvette, France

J. GIRARD

Commissariat à l'énergie atomique DAPNIA / SEA, CE Saclay, 91191 Gif sur Yvette, France

G. BARREAU, T.P. DOAN and G. PEDEMAY

Centre d'études nucléaires de Bordeaux, Domaine du Haut Vigneau, 33175 Gradignan, France

Ph. DESSAGNE and Ch. MIEHE

Centre de recherches nucléaires Strasbourg, 23 rue du Loess, BP 20 CR, 67037 Strasbourg, France

Abstract: A new isomeric state has been observed in ^{65}Ni . Its properties are described and discussed. Comparison is made with other isomers already observed in this mass region and theoretical approaches are considered.

NUCLEAR REACTION $^{64}\text{Ni}(^{18}\text{O}, ^{17}\text{O}) ^{65}\text{Ni}$, $E=72$ MeV; measured E_γ , p - γ coincidences. ^{65}Ni deduced levels, $T_{1/2}$.

1. Introduction.

As a part of an experimental program devoted to the search and study of nuclear isomerism, we used the $^{18}\text{O} + ^{64}\text{Ni}$ reaction to populate heavier Ni isotopes. Taking advantage of the spin and excitation energy selectivity offered by multi-nucleon transfer reactions, search for low spin isomers in the 65 mass region has been performed. Here, the transfer reaction channel $^{64}\text{Ni}(^{18}\text{O}, ^{17}\text{O}) ^{65}\text{Ni}$ has been selected. After the description of the experimental set-up, we present the results including information on lifetime and nuclear structure calculations are discussed.

2 Experimental technique.

The experimental procedure consists in bombarding a ^{64}Ni target with a ^{18}O ion beam, detecting and identifying the ejectile in a spectrometer and observing in coincidence, the gamma rays in a germanium array surrounding the target.

The superconducting postaccelerated tandem at Saclay delivered, for this experiment, a ^{18}O beam at 72 MeV. The beam pulse was 800 ps wide with a repetition rate of 13.5 MHz.

The ejected particles were analysed in a QDDD spectrometer set to 30° relative to the beam axis, corresponding to the grazing angle. The spectrometer has a maximum solid angle of $\Omega=14$ msr and an energy acceptance of 20%. A gas counter, filled with isobutane at a pressure of 30 torrs, placed in the focal plane, measures the energy loss (ΔE) of the ejectiles as well as their positions. Behind this chamber, the ejectiles are stopped in a large plastic scintillator coupled at both ends to phototubes connected to a meantimer system giving a time determination better than 20 ns for a selected particle. The residual energy E collected in this detector together with the ΔE allows the ejectile identification. In this experiment, we identify unambiguously $^{16,17,18}\text{O}$, $^{16,17}\text{N}$, $^{15,16,17}\text{C}$ and boron isotopes but with a lower intensity.

Our gamma detector, SAGA, is composed of six triple germanium telescopes BGO Compton suppressed. Each telescope consists of three crystals: a planar with a 10% efficiency (to detect very low gamma ray energy down to X-rays domain) and two coaxials ones with 25% efficiency each. These detectors can be used in various modes: in single mode where the frontal and the rear germaniums are used in anti-coincidence with the central one, and in sum mode where the three energies are added. For this particular experiment, SAGA was completed by the addition of four 80% efficiency germanium detectors.

The overall absolute photopic efficiency of the gamma array was measured to be $\epsilon\Omega= 0.01$ at 1.33 MeV.

3. Experimental results.

The time distribution between the ^{17}O ejectile and the gamma rays in coincidence is shown in fig. 1. Accidentals events are seen every 74 ns. For ^{17}O , the overall resolution reaches 15ns (FWHM) and allows a very drastic background rejection, typically a factor of 50 at 500 keV gamma ray energy.

The gamma rays detected by the ten detectors (6 in the SAGA array plus 4 additional), in coincidence with ^{17}O in a 48 hours run, were sorted out. The total spectrum obtained by summing the individual spectra (after gain adjustment and calibration) is shown in fig. 2 (sum mode). In this spectrum, γ -ray transitions characterizing ^{65}Ni appear as narrow lines, while the Doppler broadened humps around 870 keV and 2184 keV (arrows) correspond to the deexcitation of the first

and second excited states of ^{17}O . The list of the prominent γ lines is given in table 1. Gamma rays others than those appearing in the most recently published level schemes¹⁾ are seen, in particular at 1610, 1143 and 1013 keV. Using the gamma-gamma coincidence data obtained by J. Girard²⁾ in a $^{64}\text{Ni}(n,\gamma)^{65}\text{Ni}$ study, we can assign the 1610 keV γ -ray to the transition between the $5/2^-$ level at 1920 keV and the $3/2^-$ state at 310.4 keV. The gamma ray at 1143 keV, seen by U. Bosch et al.³⁾ is confirmed. Due to our poor γ - γ coincidence statistics, this technique does not make it possible to place the other gamma rays on the level scheme.

A two-dimensional plot of the γ -ray energies versus the γ -ray ejectile delay time (fig.3) shows that the 1013 keV γ -ray is delayed. From the analysis of its transition intensity versus the ejectile- γ delay, a half live of $26.5\text{ns} \pm 1\text{ns}$ is deduced (fig. 4). Therefore, this γ -ray signs the deexcitation of an isomeric state.

To assign the position of this 1013 keV γ -ray in the level scheme, let us examine the total excitation energy, as deduced from the kinetic energy of the ejectile measured in the QDDD, in coincidence with the 1013 keV γ -ray. As shown in fig. 5 a, three peaks could be distinguished. The first one, at 1015 ± 15 keV corresponds to the excitation of ^{65}Ni with the ejectile in its ground state. Thus, the observed 1013 keV γ -ray represents the deexcitation of this ^{65}Ni level to the ground state. A 1013 keV level with spin $9/2^+$ ^{4,5)} was already known in ^{65}Ni ; our measurement identifies its decay, (fig. 6) and establishes, for the first time, its isomeric character.

In the distribution reported in fig. 5 a, the peak observed around 1.9 MeV in the total excitation curve corresponds to the population of the isomeric state of ^{65}Ni together with the first excited state of ^{17}O ($J^\pi=1/2^+$, $E^*=870$ keV). In the peak around 4 MeV, the same Ni level is excited together with the second excited state of ^{17}O ($J^\pi=1/2^-$, $E^*=3055$ keV). Since this later peak is much wider, we have to assume an admixture of this excited state with a high energy level of ^{65}Ni feeding the 1013 keV. Hereby, we can conclude that, in this reaction, most of the observed $9/2^+$ state strength is due to direct feeding, as very few percent comes through 4 MeV excited states. This interpretation of the measured excitation spectrum is confirmed by the excitation energy spectrum in coincidence with the 870 keV γ -ray of ^{17}O (fig. 5 b). The first level is at 870 keV ($J^\pi=1/2^+$), then we find the mixture of the very intense 1013 keV of ^{65}Ni with the 870 keV, and after, the second level of ^{17}O at 3055 keV ($J^\pi=1/2^-$) and at 3840 keV ($J^\pi=5/2^-$).

The $9/2^+$ state could decay to the $5/2^+$ ground state, either through an M2 or an E3 transition. An approximate calculation in a Weisskopf frame⁶⁾ leads to predicted half-lives of 2.5 ns and 6.5 μs for such transitions, respectively. When compared

with our measured $\tau = 26.5$ ns, this transition is more likely of M2 type. It is well known that these Weisskopf estimates are not exact theoretical calculations but instead, reasonable relative comparisons between the transitions rates. This feature is seen as evidence for a rather collective character of this transition.

The existence of such an isomeric state is not unusual in this mass region. In the same experiment we also identified the already known delayed 605 keV gamma-ray in the reaction $^{64}\text{Ni}(^{18}\text{O}, ^{15}\text{C})^{67}\text{Zn}$ ⁷⁾ as well as the 563 keV and 315 keV delayed transitions in the $^{64}\text{Ni}(^{18}\text{O}, ^{16}\text{N})^{66}\text{Cu}$ reaction ⁸⁾. The configurations of the isotones ^{65}Ni , ^{67}Zn and ^{69}Ge are similar (sequence $5/2^-$, $1/2^-$, $3/2^-$, $3/2^-$, $9/2^+$). Table 2 shows the half lives measured for these isomers as well as the comparison with the Weisskopf estimates.

4. Interpretation and conclusion.

Microscopic HFB+BCS calculations with Skyrme forces are under progress ⁹⁾. They show that the $9/2^+$ state has a rather large oblate deformation ($Q_{20} = -200$ fm²) as compared to that of the almost spherical $5/2^-$ state toward which it decays ($Q_{20} = -60$ fm²). When taken into account, this difference is expected to decrease the magnitude of the matrix element of the M2 transition connecting these two states. The resulting lifetime of the $9/2^+$ is thus expected to be larger than the estimation given above ⁶⁾ which does not include deformation effects.

Hartree-Fock-Bogolyubov (HFB) calculations based on Gogny's force have also been performed ¹⁰⁾. In contrast with the earlier HFB calculations ¹¹⁾ in which TRSB (time reversal symmetry breaking) was ignored, here this is included for performing the blocking calculations for ^{65}Ni . The $9/2^+$ is a $g_{9/2}$ neutron quasi-particle with quadrupole mass moment $Q_{20} = -204$ fm², while the predicted g.s. level is $\nu 2\pi 2$ with $Q_{20} = 0$. The excitation energy of the predicted $g_{9/2+}$ is $E_x = 719$ keV, slightly below the experimental value ($E_x = 1013$ keV). These calculations suggest shape coexistence phenomena.

The identification of the isomeric state at 1013 keV in ^{65}Ni impulsed new theoretical developments that are under progress. In order to have a complete understanding of this isomeric state, a full microscopical description of both wave functions and transitions is needed. Such calculations will allow to determine how the shape change affects the lifetime of this state.

The experimental procedure used here, namely the association of an efficient γ detection array with a high resolution spectrometer, revealed itself to be well suited for this kind of investigation. Our technique allows, in particular, the

precise location of the γ transition of interest in the level scheme, as well as its lifetime determination. It is therefore promising for the search of shape isomeric states.

We would like to thank Prof. C. Bourgeois and the Institut National de Physique Nucléaire et de Physique des Particules (IN2P3) for providing the four extra germanium detectors (two belonging to the EUROGAM collaboration and two borrowed from the Château de Cristal array).

REFERENCES

- 1) Nuclear Data Sheets Vol. 69, 2, 1993
- 2) J. Girard, Note CEA-N-1500 (1972)
- 3) U. Bosch, W.D. Schmidt-Ott, E. Runte, P. Tidemand-Petersson, P. Koschel, F. Meissner, R. Kirchner, O. Klepper, E. Roeckl, K. Rykaczewski, and D. Schardt, Nucl. Phys. A477 (1988) 89
- 4) T.R. Anfinsen, K.Bjorndal, A. Graue, J.R. Lien, G.E. Sandvik, L.O. Tveita, K.Ytterstad and E.R. Cosman, Nucl. Phys. A157 (1970) 561
- 5) M. Turkiewicz, P. Beuzit, J. Delaunay and J.P. Fouan, Nucl. Phys. A143 (1970) 641
- 6) J.M. Blatt, V.F. Weisskopf, in Theoretical Nuclear Physics (J.Wiley and sons, 1952) p. 623
- 7) U.Bertschat, U. Leithauser, K.H. Maier, E. Recknagel, B. Spellmeyer, Nucl. Phys. A215 (1973) 486
- 8) J. Bleck, R. Butt, K.H. Lindenberger, W. Ribbe and W. Zeitz, Nucl. Phys. A197 (1972) 620
- 9) R. Mehrem, P. Bonche, P.H. Heenen, private communication
- 10) M. Girod, private communication
- 11) M. Girod, Ph. Dessagne, M. Bernas, M. Langevin, F. Pougheon and P. Roussel, Phys. Rev. C37 (1988) 2600

Figure captions

Fig.1. Time spectrum obtained in $^{64}\text{Ni}(^{18}\text{O}, ^{17}\text{O}) ^{65}\text{Ni}$ reaction.

Fig.2. Total gamma spectrum measured in $^{64}\text{Ni}(^{18}\text{O}, ^{17}\text{O}) ^{65}\text{Ni}$ reaction. Arrows indicate the Doppler broadened ^{17}O γ -rays.

Fig.3. Gamma-ray energies versus gamma-ejectile delay for $^{64}\text{Ni}(^{18}\text{O}, ^{17}\text{O}) ^{65}\text{Ni}$ reaction.

Fig.4. Intensity of the 1013 keV γ transition as function of time.

Fig.5. a) Excitation energy spectrum measured in the QDDD in coincidence with the 1013 keV γ -ray.

b) Excitation energy spectrum measured in the QDDD in coincidence with the 870 keV γ -ray (first excited state of ^{17}O).

Fig.6. ^{65}Ni level scheme obtained in this experiment.

Table Captions.

Table 1. Gamma-ray energies and corresponding intensities measured in this experiment. The intensities are normalized to the first level at 310 keV.

Table 2. Comparison of the half-lives (theoretical and experimental) of ^{65}Ni isotones having the same level configuration. The same quantities are also reported for ^{66}Cu .

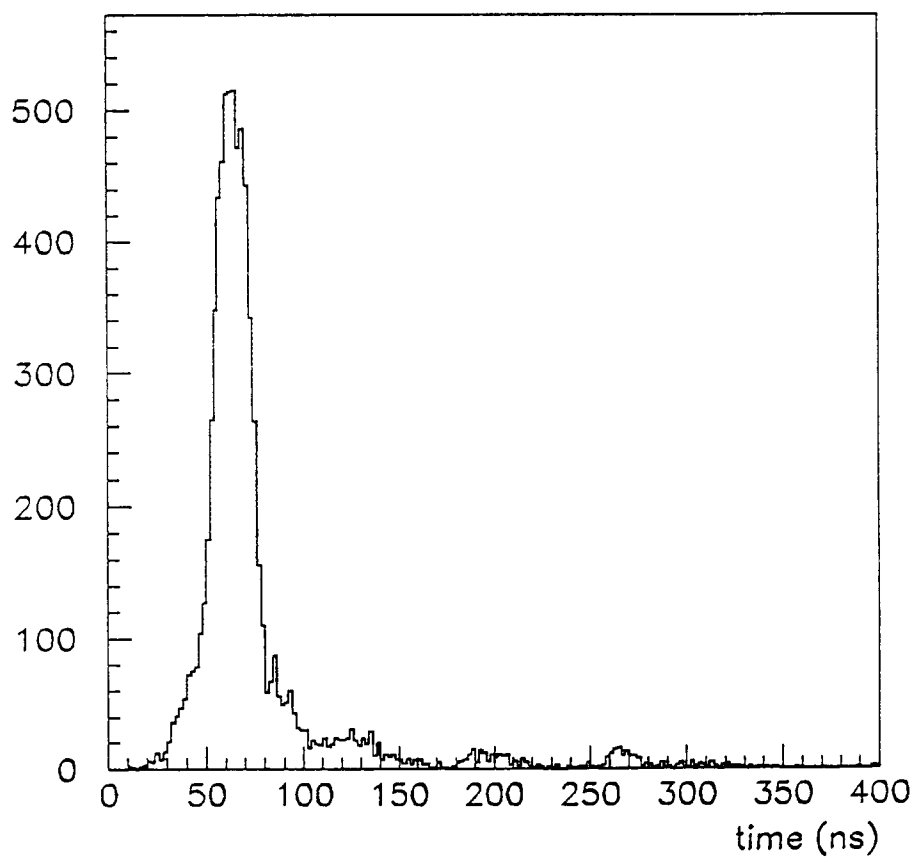


Fig. 1

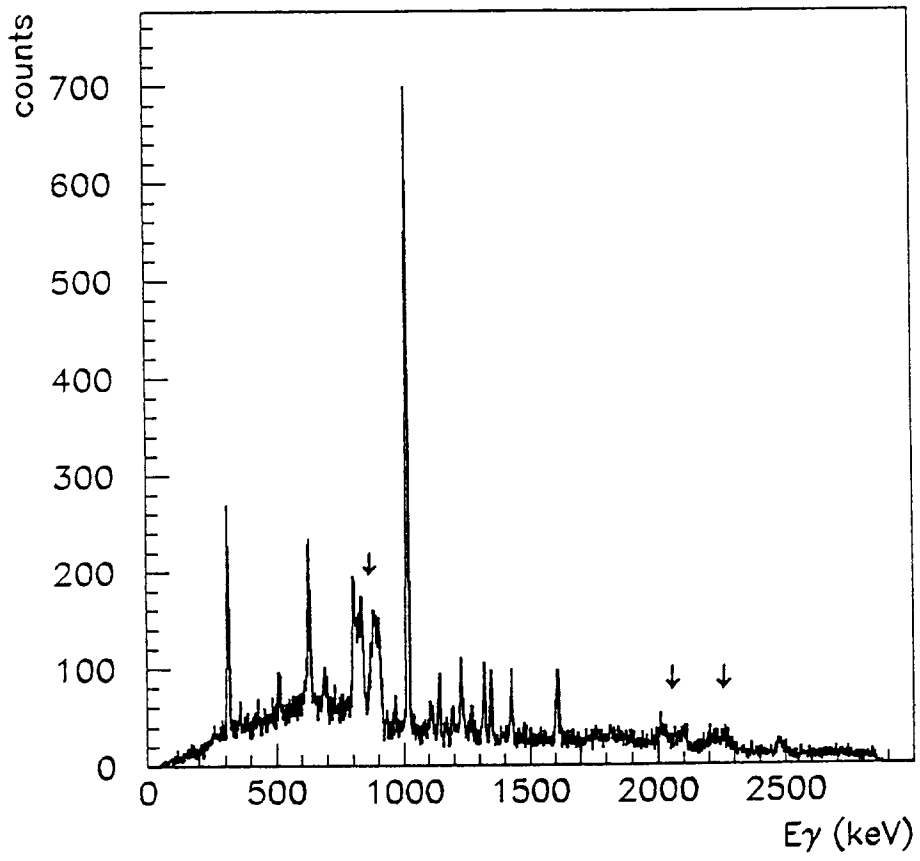


Fig. 2

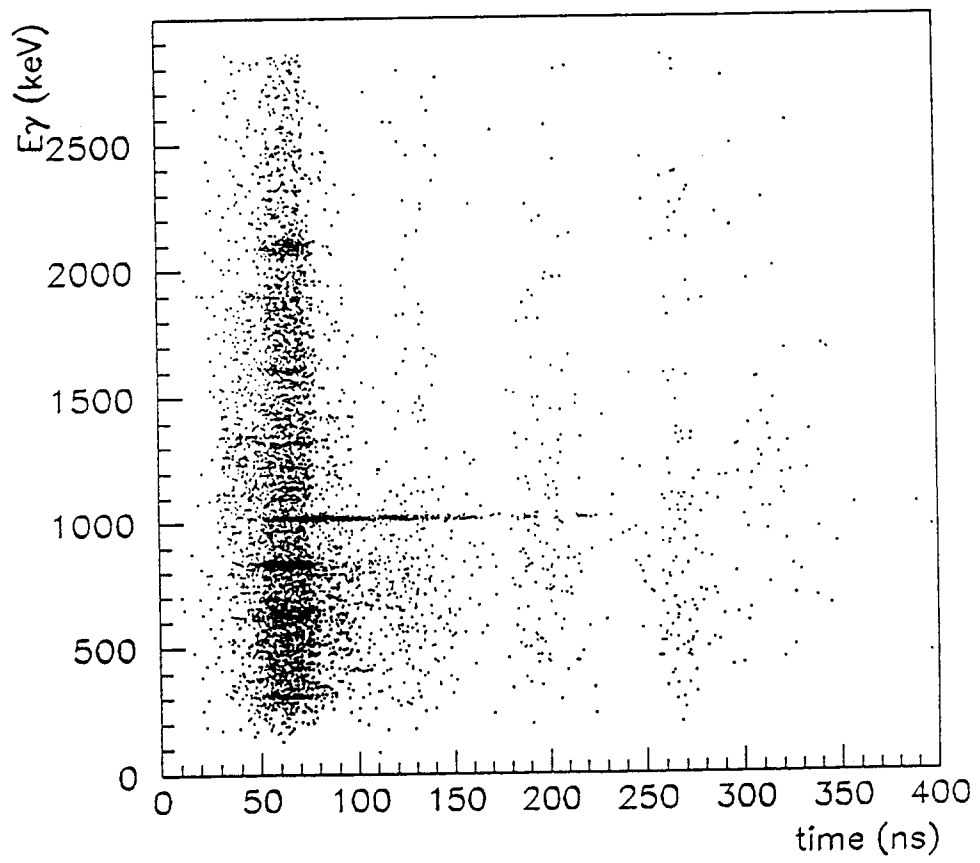


Fig. 3

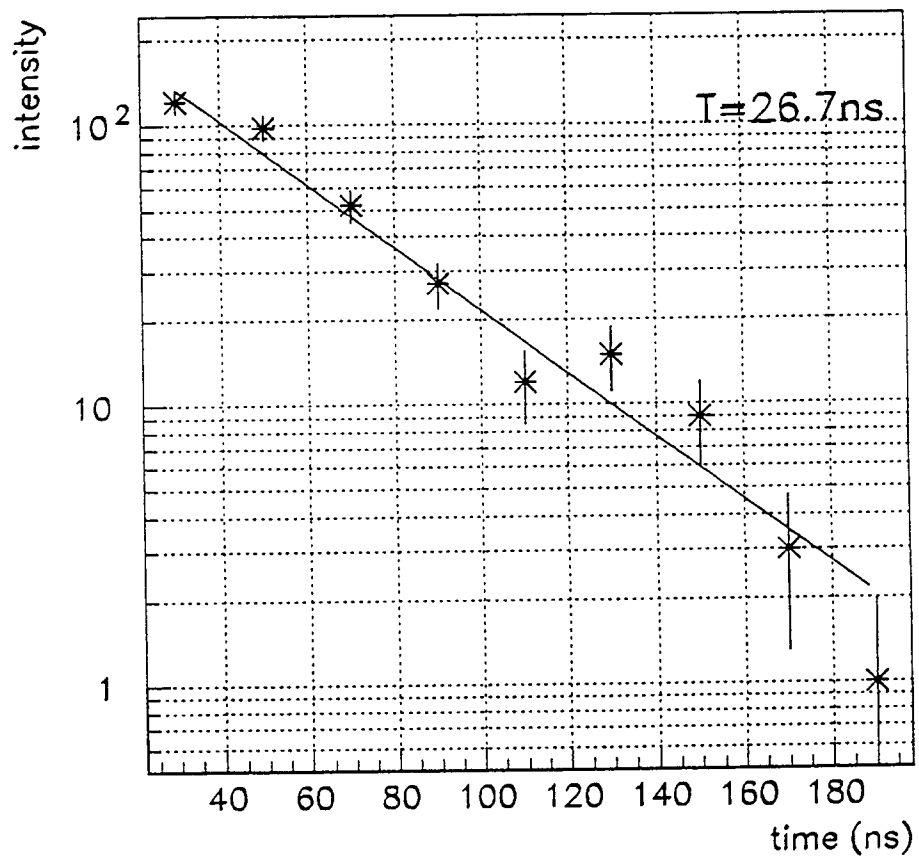


Fig. 4

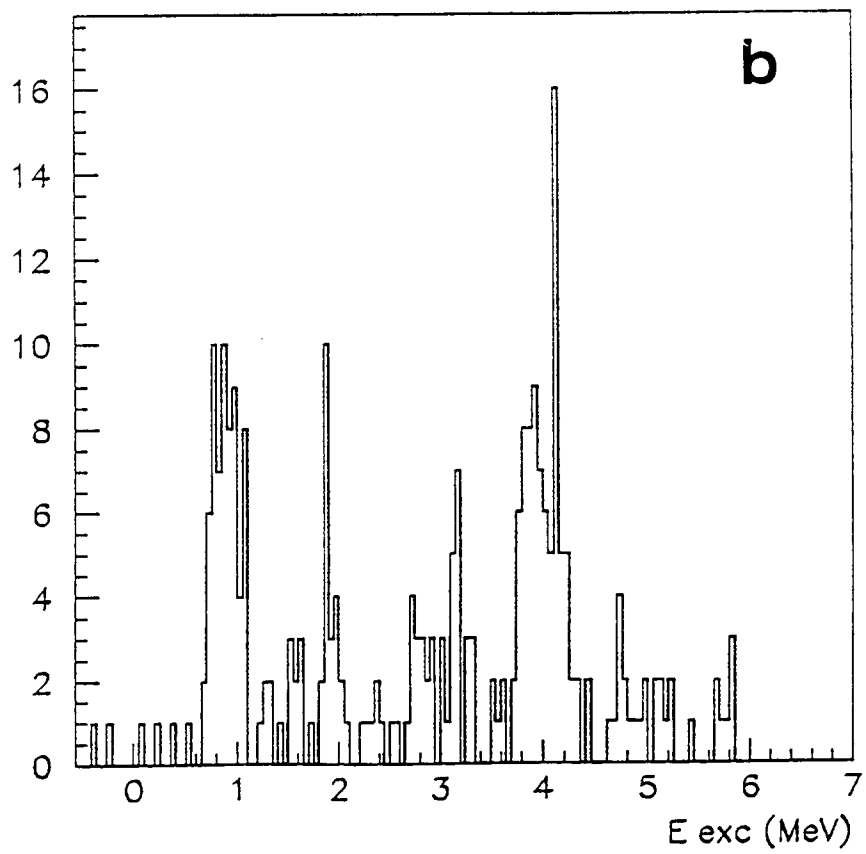
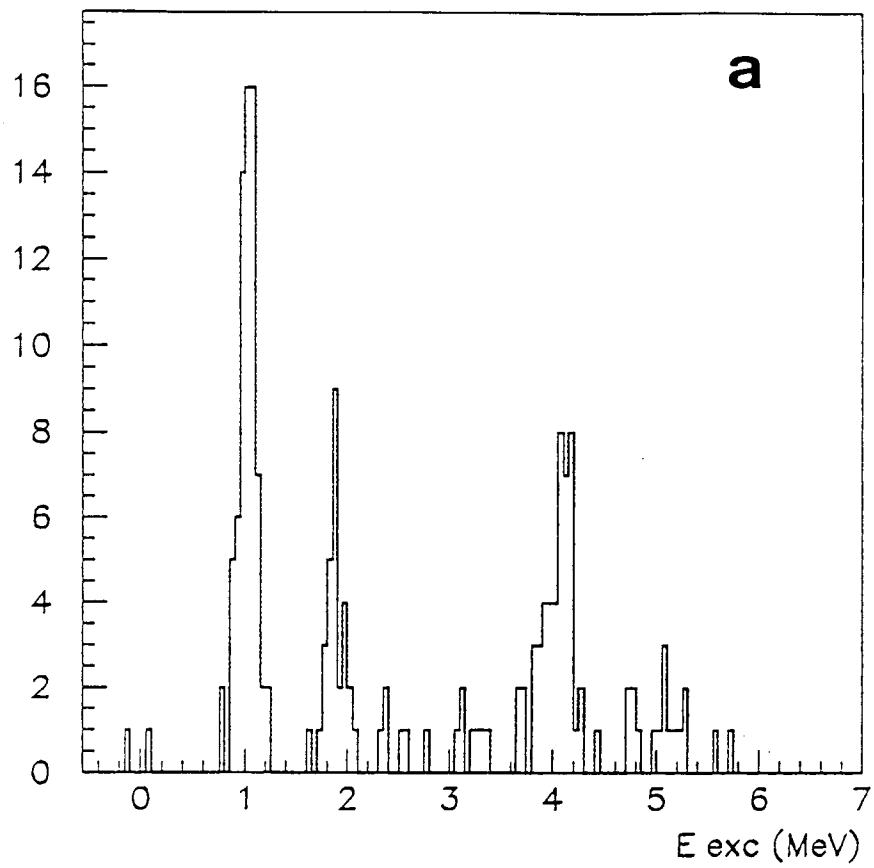


Fig. 5

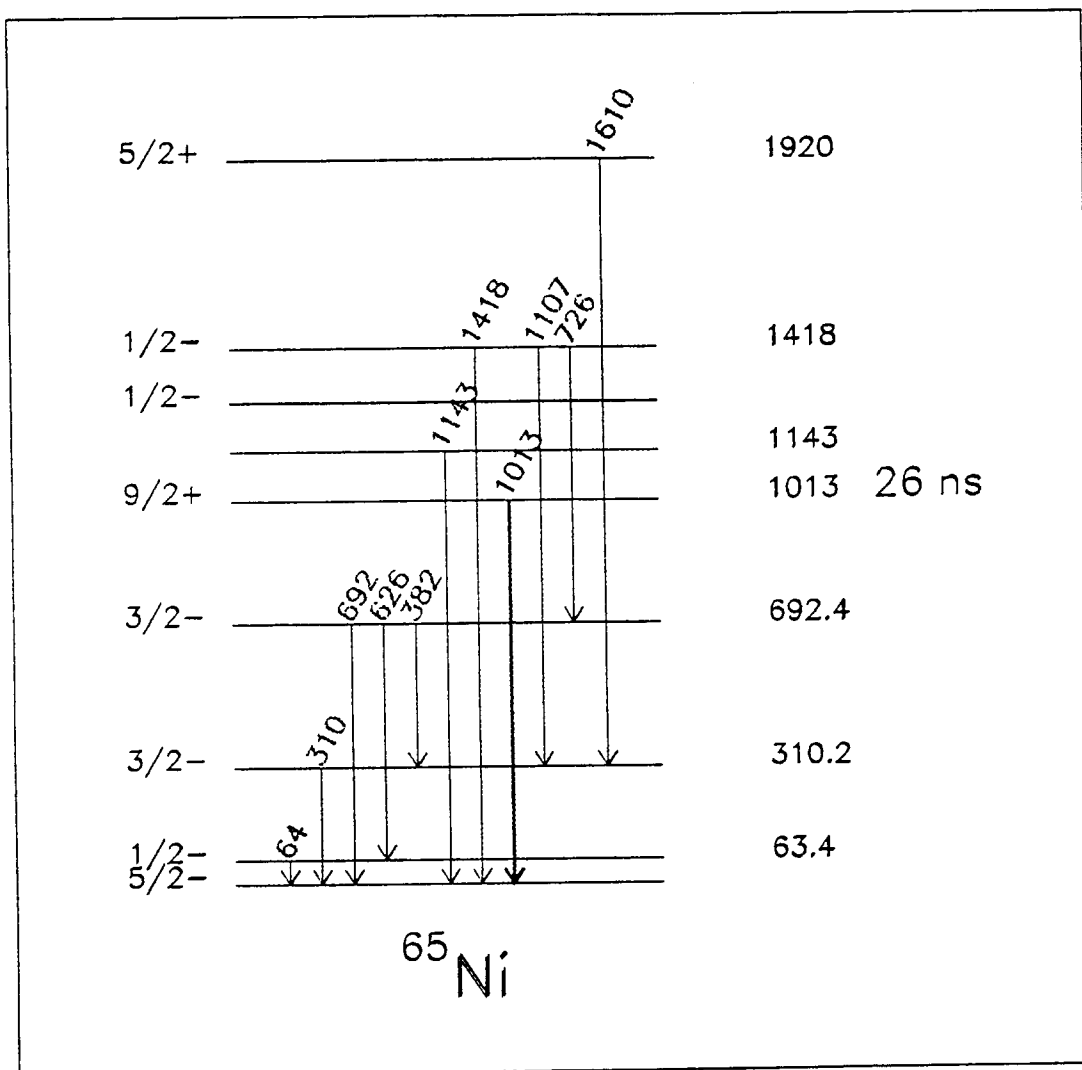


Fig. 6

Table 1

	E_γ (keV)	$T_{1/2}$ exp	$T_{1/2}^{th}_{(M2)}$	T_{exp}/T_{th}	Trans
$^{65}_{28}\text{Ni}_{37}$	1013	26 ns	2.5 ns	10.4	9/2+ 5/2-
$^{67}_{30}\text{Zn}_{37}$	604	333 ns	34 ns	9.8	9/2+ 5/2-
$^{69}_{32}\text{Ge}_{37}$	398	2800 ns	269 ns	10.4	9/2+ 5/2-
$^{66}_{29}\text{Cu}_{37}$	563	600 ns	49.2 ns	12.2	6- 4+

Table 2

E_γ (keV)	Level (keV)	Spin Parity	Intensity (%)
310 (3)	310 (5)	$3/2^-$	100. (<i>normalized</i>)
567 (3)			14 (1.0)
629 (3)	692.4 (6)	$3/2^-$	100 (7.0)
693 (3)		$3/2^-$	21 (1.2)
726 (4)	1418.1 (7)	$1/2^-$	7 (0.5)
962 (4)	1273. (10)	$1/2^-$	5 (0.4)
1013 (3)	1013. (10)	$9/2^+$	280 (10)
1107 (4)	1418.1 (7)	$1/2^-$	9 (0.7)
1143 (4)	1143. (10)		22 (2.0)
1166 (4)			3 (0.5)
1194 (4)			15 (1.0)
1225 (3)			33 (2.4)
1265 (3)			14 (3.0)
1319 (3)			43 (3.0)
1344 (3)			28 (2.2)
1388 (6)			4 (0.3)
1418 (4)	1418.1 (7)	$1/2^-$	5. (0.4)
1426 (6)			5 (0.4)
1474 (6)			2 (0.5)
1501 (6)			4 (0.4)
1610 (5)	1920.3 (8)	$5/2^+$	48 (4.0)
1815 (5)			7 (0.5)
1901 (5)			8 (0.6)
2475 (5)			

